Ceramics International 42 (2016) 8234–8239

Contents lists available at ScienceDirect

Ceramics International

journal homepage: www.elsevier.com/locate/ceramint

Room-temperature large magnetocaloric effect and critical behavior in $La_{0.6}Dy_{0.1}Sr_{0.3}MnO_3$

Lisha Xu [a], Lili Chen [a], Jiyu Fan [a,*], Klaus Bärner [b], Lei Zhang [c], Yan Zhu [a], Li Pi [c], Yuheng Zhang [c], Daning Shi [a]

[a] Department of Applied Physics, Nanjing University of Aeronautics and Astronautics, Nanjing 210016, China
[b] Department of Physics, University of Göttingen, Tammanstrasse 1-37077, Göttingen, Germany
[c] High Magnetic Field Laboratory, Chinese Academy of Sciences, Hefei 230031, China

ARTICLE INFO

Article history:
Received 18 January 2016
Received in revised form
3 February 2016
Accepted 4 February 2016
Available online 12 February 2016

Keywords:
D. Manganite
E. Magnetocaloric effect
C. Phase transitions

ABSTRACT

The effect of dysprosium incorporation in $La_{0.7}Sr_{0.3}MnO_3$ perovskite manganite on its magnetic properties, magnetocaloric effect and critical behavior was investigated. The temperature dependent magnetization data exhibit a sharp paramagnetic–ferromagnetic transition at T_C=307 K, which nature has been identified to be a second-order transition by the scaling laws for magnetocaloric effect. The maximum magnetic entropy change and the relative cooling power are found to be, respectively, 8.314 J/kg K and 187 J/kg for a 5 T magnetic field change without a hysteresis loss, making this material a promising candidate for magnetic refrigeration at room temperature. To study the critical behavior of the paramagnetic–ferromagnetic transition, some related critical exponents (β, γ, and δ) have been also calculated. The values of critical exponents indicate that the present phase transition does not belong to the common transition classes but shows some abnormal variation. We suggest that the induced lattice disordering and magnetic disordering due to Dysprosium incorporation are essential reasons for the presence of a large magnetocaloric effect and of an anomalous ferromagnetic phase transition in the present material

1. Introduction

Over the past few years, magnetic refrigeration in room-temperature range has attracted global interest owing to its energy-efficient and environment-friendly advantages over the gas compression–expansion refrigeration techniques [1,2]. This subject is based on the magnetocaloric effect (MCE) which is an intrinsic property of magnetic materials. The MCE is defined as the thermal responses (heating or cooling) of magnetic solids during the application or removal of external magnetic field. In general, MCE is considered as the entropy change of the system in an isothermal magnetization process [3]. Nowadays, the majority of magnetic refrigeration research mainly concentrates on exploring some suitable materials which are cost-effective but exhibit a relative large isothermal entropy change at a wide temperature range. Large MCE was firstly reported in the materials with the first-order magnetic transition, such as the ternary compound $Gd_5Si_2Ge_2$ by Pecharsky and Gschneidner [4] and $LaFe_{13-x}Si_x$ by Shen et al. [5]. However, the first-order magnetic transition is always accompanied with the appearance of thermal hysteresis and field hysteresis upon variation in magnetization with temperature and magnetic field which inevitably causes energy loss and decreases the refrigerant capacity (RC) [6]. Additionally, the first-order magnetic transition generally occurs in a narrower temperature range, which also results in a smaller RC. Therefore, exploration for new magnetic refrigeration has recently shifted to the composite materials of the second-order magnetic transition. Although the second-order phase transition does not produce a larger entropy change compared with the first-order transition, a broader temperature and non-thermal hysteresis can induce more considerable RC.

With a large MCE reported in the second-order magnetic transition $La_{1-x}Ca_xMnO_3$ [7], the perovskite oxides have been intensively studied due to their distinct advantages, such as chemical stability, low production cost, high resistivity than intermetallic alloy (minimum eddy current loss), and a broader temperature range of magnetic phase transition. The large MCE has been recently reported in other perovskite manganites with the different compositions as well [8–13]. Generally, a sharp paramagnetic–ferromagnetic (PM–FM) phase transition and a large spontaneous magnetization [14] are the necessary prerequisites for magnetic materials to have a considerable MCE. In addition, it has been also demonstrated that the magnetocaloric parameters are dependent

* Corresponding author. Tel.: +86 25 52075729; fax: +86 25 83336919.
E-mail address: jiyufan@nuaa.edu.cn (J. Fan).

http://dx.doi.org/10.1016/j.ceramint.2016.02.035
0272-8842/

on the applied magnetic field and associated with the intricate nature of magnetic phase transition which can be parametrized by critical exponents governing the transitions [15]. The analysis of critical behavior can provide significant information about the thermodynamic observations near T_C. Therefore, in this paper, we used the heavy rare-earth metal dysprosium to partially replace lanthanum to investigate MCE and critical behavior of $La_{0.6}Dy_{0.1}Sr_{0.3}MnO_3$ (LDSMO). It is well known that the pristine $La_{1-x}Sr_xMnO_3$ is a typical perovskite manganite which physical properties depend highly on the doping content x and the largest MCE occurs at the optimal doping level of $x=0.3$ [16,17]. These effects are usually attributed to the interplay between spin, lattice, charge and orbital degrees of freedom [18,19]. In view of a sizable magnetic moment of Dy^{3+} ion (10.6 μ_B), we think that a slight Dy-substitution for La not only augments some extra magnetic interactions or causes less magnetic disordering, but also does not remarkably change the double-exchange effect taken place on the B-site sublattices, which is mainly responsible for the magnetic interaction in this system. As an external magnetic field is applied on it, a large magnetic disordering–ordering transition maybe occurs and a considerable magnetic entropy change is possibly observed. Our results show that $La_{0.6}Dy_{0.1}Sr_{0.3}MnO_3$ has a large value of MCE and high relative cooling power (RCP), which strongly suggests that this compound may also be considered as a potential candidate for room-temperature magnetic refrigeration applications. Meanwhile, we find that the obtained critical exponents in LDSMO do not belong to the common university classes and their variations are not also subjected tothe general ruler. We think that the induced crystal disordering on A-site lattice and magnetic disordering on B-site lattice due to the dysprosium substitution are the driving force for generating large MCE in LDSMO, which are also related to the abnormal critical exponents observed in this sample.

2. Experiment

A polycrystalline LDSMO sample was prepared by traditional solid state reaction method. The structure and phase purity of the sample were checked by powder X-ray diffraction (XRD) using Cu Kα radiation at room temperature. The XRD patterns prove that the sample is pure and a single-phase with orthorhombic structure. The magnetization versus temperature and magnetization versus magnetic field were measured by using a Magnetic Property Measurement System (Quantum Design MPMS 7T-XL) with a superconducting quantum interference device (SQUID) magnetometer.

3. Results and discussion

Fig. 1 shows the temperature dependence of magnetization (M–T) measured under the magnetic field of 0.01 T, which exhibits a sharp PM–FM phase transition. The transition temperatures were determined from the linear fitting of M^{-1} vs. T curve using the Curie–Weiss Law $\chi=C/(T-\theta_P)$ (C is the Curie constant and θ_P is the Weiss temperature), as shown in the right axis of Fig. 1. Clearly, the relationship between M^{-1} and T preferably follows the Curie–Weiss Law and the Weiss temperature θ_P is deduced to be about 307 K. The positive value of θ_P confirms the existence of FM exchange interaction in this sample. Based on the data of Curie constant obtained from the above fitting, the effective PM moment ($P_{eff}=2.83\sqrt{C}$) is determined to be $P_{eff}=2.5$ μ_B. The inset shows the isothermal M–H curve measured at 5.0 K. The magnetization increases sharply and then tends to saturation as the applied magnetic field reaches $\mu_0H=0.6$ T. The saturated magnetization (M_S) can be obtained from an extrapolation of the high field M–H curve

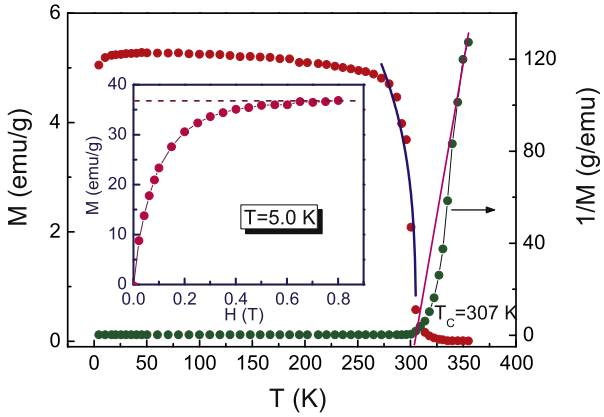

Fig. 1. Left axis: temperature dependence of magnetization measured at $H=100$ Oe and the solid line represents the fitting data according to the scaling law $M \sim (T_C - T)^{\beta}$. Right axis: inverse magnetization as a function of temperature for $La_{0.6}Dy_{0.1}Sr_{0.3}MnO_3$ and the solid line represents the fitting data according to the Curie–Weiss law. Inset shows isothermal magnetization at 5.0 K. (For interpretation of the references to color in this figure caption, the reader is referred to the web version of this paper.)

to $\mu_0H=0$, and the obtained M_S is 1.51 μ_B. According to Rhodes–Wohlfarth criterion [20], the degree of itinerancy can be determined from the ratio of P_{eff} to M_S. The ratio is close to one for the localized moment whereas it is larger than one for the itinerant moment. Here, the ratio of 1.66 implies that the LDSMO electrons possess an itinerant character.

Although the pristine $La_{0.7}Sr_{0.3}MnO_3$ is an optimal ferromagnetic material and shows colossal magnetoresistance effect, the periodic arrangement of Mn^{3+}/Mn^{4+} ions on the B-site sublattice can be disrupted by the Dy^{3+} ions substitution on the A-site sublattice. Along with the local lattice distortion contributed by Jahn–Teller active Mn^{3+} ions, the size mismatch among La^{3+}, Dy^{3+} and Sr^{2+} ions changes the Mn^{3+}–O^{2-}–Mn^{4+} bond angle and Mn–O bond length, converting a periodic arrangement into a disordering one of Mn^{3+}/Mn^{4+}. Therefore, the A-site substitution influences the B-site magnetic interaction. Here, the Dy^{3+} incorporation brings some new magnetic behaviors different from that in pristine $La_{0.7}Sr_{0.3}MnO_3$. Generally, the spontaneous magnetization below T_C can be depicted by the scaling law $M \sim (T_C - T)^{\beta}$ [21]. As shown in Fig. 1, the blue solid lines represent the fitted result by using this formula and the critical exponent β is deduced to be 0.4799 which has a noticeable discrepancy from the normal value of $\beta=0.5$ in mean-field model. This obvious discrepancy will allow us to further consider the role of the Dy^{3+} substitution how to influence the magnetic phase transition in LDSMO. In the previous investigation, it has been reported that the A-site substitution with large magnetic moment causes some precursor effects which mainly show as the extra contribution to resistivity and magnetization over a wide temperature range above the long range magnetic ordering [22,23]. Since the MCE is the measure of variation in magnetic moments configuration, we can estimate that the precursor effect due to Dy^{3+} substitution undoubtedly influences the MCE in LDSMO.

To understand this influence on MCE, we investigate its MCE which can be determined through calculating isothermal magnetic entropy change (ΔS_M) using the Maxwell relation for materials that undergo a second-order magnetic transition:

$$\Delta S(T, H) = S_M(T, H) - S_M(T, 0) = \int_0^H \left(\frac{\partial M(T, H)}{\partial T}\right) dH \quad (1)$$

In practice, the magnetic entropy change $|\Delta S_M|$ can be evaluated from the isothermal magnetization measured with small temperature

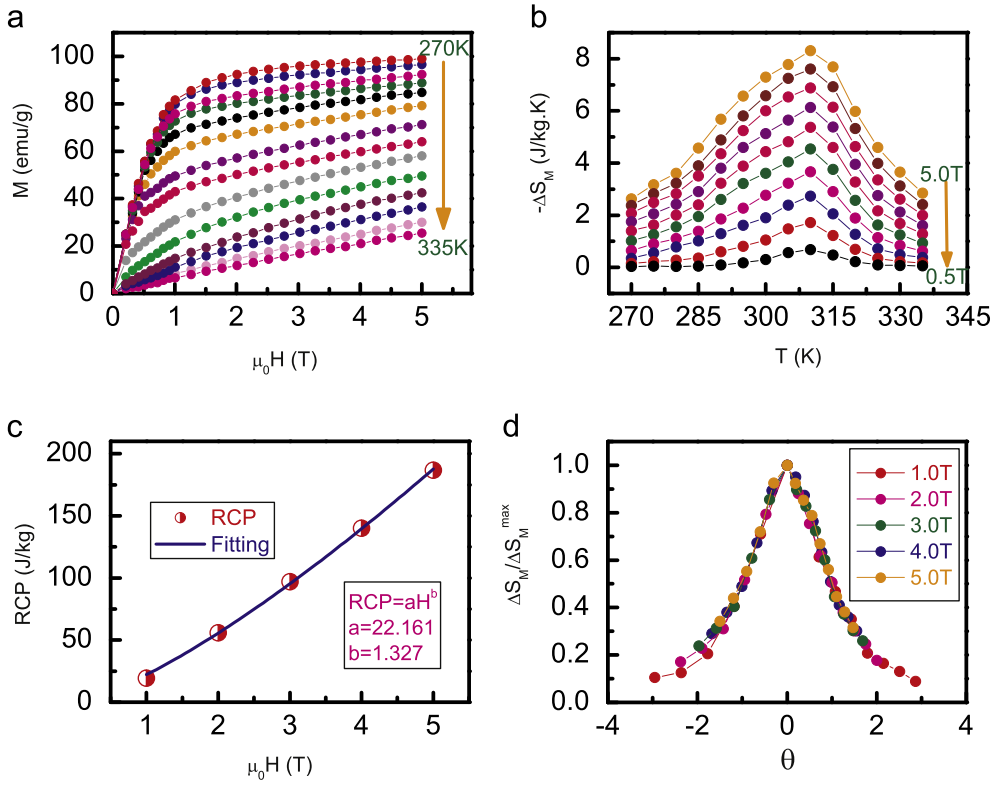

Fig. 2. (a) Isothermal magnetization measured at different temperatures for $La_{0.6}Dy_{0.1}Sr_{0.3}MnO_3$. (b) Magnetic entropy change $-\Delta S$ plotted as a function of temperature at different applied fields. (c) Refrigerant capacity as a function of applied magnetic field and the solid line is the fitting results following RCP$=aH^b$. (d) Normalized magnetic entropy change dependence of the rescaled temperatures.

intervals, where $\Delta S_M(T, H)$ can be approximated as

$$|\Delta S_M| = \sum \frac{M_i - M_{i+1}}{T_{i+1} - T_i} \Delta H_i \quad (2)$$

where M_i and M_{i+1} are the experimental data of the magnetization at T_i and T_{i+1}, respectively, under a magnetic field H_i. Fig. 2(a) represents the magnetic field dependence of magnetization at various temperatures between 270 and 335 K. By using Eq. (2) and isothermal magnetization in Fig. 2(a), the ΔS_M vs. T under different magnetic fields are presented in Fig. 2(b). As expected, the ΔS_M depends on both the applied magnetic field and the temperature. ΔS_M increases and reaches a maximum value (ΔS_{max}) when the temperature approaches the Curie temperature. In fact, the magnetic entropy changes dependence on the value of $(\partial M/\partial T)_H$ has been clearly indicated in Eq. (1). Therefore, the large magnetic entropy changes usually occurs near T_C where magnetization changes swiftly with variation of temperature. Furthermore, the effect may be further maximized as the variation in magnetization with respect to temperature appear in a narrow temperature interval [24]. Similar to the above analysis, the data of ΔS in Fig. 2(b) indicates that this sample possesses a large magnetocaloric effect. Here, the maximum magnetic entropy change ΔS_{max} is about 8.314 J/kg K with the magnetic field variation of ΔH = 5.0 T. As important result from our research work, it should be noticed that maximum magnetic entropy in present material is near to that found in Gd (10.20 J/kg K under 5 T) [1]. So, it is large enough to be used for magnetic refrigeration at room-temperature. Meanwhile, a comparison between our results and other magnetocaloric materials is also presented in Table 1.

In magnetic refrigeration technology, RCP is another meaningful parameter for determining the cooling power of a material with MCE [25]. RCP can be defined as:

$$RCP = -\Delta S_{max}\, \delta T_{FWHM} \quad (3)$$

Table 1
Experimental values of T_C, magnetic field variation ΔH, magnetic entropy change $|\Delta S|$, relative cooling power (RCP) for our $La_{0.6}Dy_{0.1}Sr_{0.3}MnO_3$ sample compared with those for Gd and some typical manganites exhibiting the giant MC effect near room temperature, with magnetic-field variations up to 50 kOe.

Material	T_C (K)	ΔH (T)	$\|\Delta S\|$ (J/kg K)	RCP (J/kg)	Ref.
Gd	295	5.0	10.2	410	[1]
$La_{0.6}Dy_{0.1}Sr_{0.3}MnO_3$	307	5.0	8.314	187	Present
$La_{0.7}Sr_{0.3}MnO_3$	370	5.0	5.15	252	[45]
$La_{0.7}Ca_{0.3}MnO_3$	264	5.0	7.7	–	[46]
$La_{0.67}Ba_{0.33}MnO_3$	292	5.0	1.48	161	[47]
$La_{0.7}Ca_{0.2}Sr_{0.1}MnO_3$	308	5.0	7.5	374	[48]
$Pr_{0.63}Sr_{0.37}MnO_3$	300	5.0	8.52	511	[49]

where δT_{FWHM} is the full width at half maximum of the magnetic entropy change curve. As shown in Fig. 2(c), the value of RCP increases with applying magnetic field. For ΔH = 5.0 T, RCP reaches about 187 J/kg, which is comparable to that reported for many other manganites, as shown in Table 1. The obtained RCP increases with the applied magnetic field indicating that RCP is strong field dependent. In fact, RCP depends on magnetic field (H) according to a power law form RCP$=aH^b$. [26]. As shown in Fig. 2(c) (solid lines), the fitting value of b was obtained to be ~1.327, which approximates to reported other results [27,28].

Apart from the above discussion of MCE and RCP, in the following section, we will study the critical behavior of PM–FM phase transition in LDSMO. Generally, the order of magnetic phase transition can be determined with the criterion suggested by Banerjee [29]. (Negative and positive slope of H/M vs. M^2 curves respectively correspond to a first-order and second-order transition.) However, a more accurate method has been recently proposed by Franco et al., in which a phenomenological universal

curve of the field dependence of the magnetic entropy change can more accurately distinguish the order of the magnetic phase transition [30,31]. This suggestion is based on the assumption that, if such universal curve exists, all other curves measured under different applied magnetic fields should collapse on the same universal curve in the case of a second-order phase transition. In contrast, for materials with a first-order phase transition, the scaled curves do not follow a universal behavior. Here, this method was used to judge the order of PM–FM phase transition occurred in the present sample. The concrete steps are performed according to the following protocol. First, two points are selected from each ΔS_M vs. T curves. One (T_{r1}) is below T_{peak} and the other (T_{r2}) is above T_{peak}. Both of them satisfy the relation $\Delta S_M(T_{r1}) = \Delta S_M(T_{r2}) = k\Delta S_M^{peak}(T_{peak})$, where ΔS_M^{peak} is the maximum value of the selected ΔS_M vs. T curves and k is the relative value of the entropy changes at two reference temperatures T_{r1} and T_{r2}. In general, the selection of k value is arbitrary but k value is always between 0 and 1. Here, we choose the $k=0.5$ to construct the universal master curve. Then, two reference temperatures are used here and the temperature axis is rescaled as:

$$\theta = \begin{cases} \theta_- = (T_{peak} - T)/(T_{r1} - T_{peak}), & T < T_{peak} \\ \theta_+ = (T - T_{peak})/(T_{r2} - T_{peak}), & T > T_{peak} \end{cases} \quad (4)$$

As shown in Fig. 2(d), all the ΔS_M vs. T curves collapse into a single curve. This result indicates that the observed PM–FM phase transition in Fig. 1 is a second-order transition.

For a second-order phase transition, its thermodynamic function can be expressed by a power law form with three critical exponents [32,21], namely, β, γ, and δ. Meanwhile, δ is associated with the critical magnetization isotherm at T_C ($M \propto H^{1/\delta}$), which can be deduced by fitting $M(H)$ curve at T_C. As the actual phase transition temperature is the unknown, two different $M(H)$ curves are chosen to deduce δ. One is at 305 K and the other is at 310 K. Both temperatures are the nearest temperature approached to actual T_C. The values of δ are 3.8632 and 2.523 for $T=305$ and 310 K, respectively. By comparison, we found that the $\delta=2.523$ is too small and is not up to the actual phase transition. Therefore, the fitting value of 310 K was excluded. Fig. 3(a) only presents the fitting curve at 305 K. According to the mean-field theory, the regular Arrott plot (H/M vs. M^2 curve) with $\beta=0.5$ and $\gamma=1.0$ near the transition regime should be a set of parallel lines in the high field regimes, and the line at T_C should pass through the origin [33]. The regular Arrott plot was shown in Fig. 3(b). However, the nonlinear and curvature characters in the Arrott plot indicate that mean field model with $\beta=0.5$ and $\gamma=1.0$ is not completely valid. Moreover, the line at 305 does not pass through the origin. Therefore, the Arrott plot should be replotted with the modified critical exponents. According to the Widom scaling relation [34], three critical exponents (β, γ, and δ) are related through the following formula:

$$\delta = 1 + \frac{\gamma}{\beta} \quad (5)$$

By using the obtained critical exponents $\beta=0.4799$ and $\delta=3.8632$, we can deduce the value of γ to be 1.374. Then, a modified Arrott plot was shown in Fig. 3(c). It is found that the modified critical exponents yield quasi-straight lines at high fields for LDSMO. The line at 305 K just passes through the origin. For further comparison, in the inset of Fig. 3(c), we calculate the relative slope RS (RS $\equiv S(T)/S(T_C)$) as the function of temperature, where $S(T)$ is the slope of the quasi-straight line in high field region at different temperatures. In the most ideal case, all RSs should be equal to 1 because the most suitable modified Arrott plot is a series of parallel straight lines [35]. Obviously, the RS deduced form Fig. 3(c) (solid symbol) is better than that deduced from Fig. 3(b) (open symbol). However, as listed in Table 2, we can notice that the deduced exponents do not completely agree with any of the conventional universality classes. So we need to check the accuracy of the deduced exponents. It can be done with the

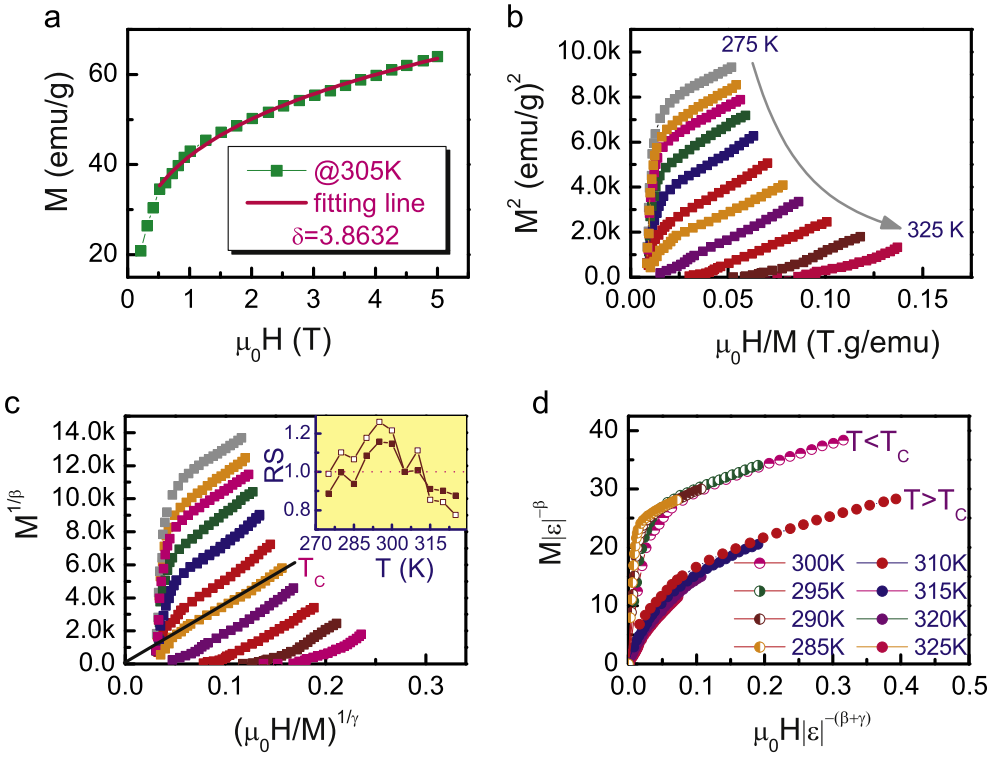

Fig. 3. (a) Isothermal magnetization $M(H)$ at T_C and the solid line is the fitting results. (b) Arrott plots of isotherms M^2 vs. H/M at different temperatures. (c) Isothermals of $M^{1/\beta}$ vs. $H/M^{1/\gamma}$ with modified critical exponents and inset shows the normalized slopes [RS=$S(T)/S(T_C)$] as a function of temperatures. (d) Scaling plots of renormalized magnetization M vs. renormalized field H above and below T_C.

Table 2
Comparison of critical exponents of $La_{0.6}Dy_{0.1}Sr_{0.3}MnO_3$ (LDSMO) with different theoretical models.

Composition	β	γ	δ	Ref.
LDSMO	0.4799	1.374	3.8632	Present
3D-XY	0.346	1.316	4.81	[36]
3D-Ising	0.325	1.24	4.82	[36]
Mean-field	0.5	1.0	3.0	[36]
3D-Heisenberg	0.365	1.386	4.8	[36]
Tricritical mean-field	0.25	1.0	5.0	[44]

prediction of the scaling hypothesis:

$$M(H, \varepsilon) = \varepsilon^{\beta} f_{\pm}(H/\varepsilon^{\beta+\gamma}) \quad (6)$$

where $f_{\pm}$ are fare regular functions with f_{+} and f_{-} being for above and below T_C, respectively [36]. The scaling relation claims that $M(H, \varepsilon)\varepsilon^{-\beta}$ vs. $H/\varepsilon^{\beta+\gamma}$ should yield two universally different branches, one for $T > T_C$ and the other for $T < T_C$. Taking the values of β and γ from above, the isothermal magnetization around T_C are plotted in Fig. 3(d). It is clear that all the magnetization data fall into two sides: one for $T > T_C$ and the other for $T < T_C$. The obedience of scaling equation over the entire range of normalized variables indicates that the obtained critical exponents are reliable and consistent with the scaling hypothesis.

In order to manifest the influence of critical exponents on MCE, the magnetic field dependence of magnetic entropy change has been examined. From Fig. 2(a), the magnetic field dependence of isothermal entropy change at the individual temperatures can be deduced. Obviously, as shown in Fig. 4(a), all the entropy changes reveal a monotonic increase with the applied magnetic field at different temperatures. Franco and co-workers [3] proposed a power function to elucidate the magnetic field dependence of the maximum magnetic entropy change ($\Delta S_{max} \approx a(\mu_0 H)^n$). They introduced a magnetic-order parameter varying as a function of T and H

$$n(T, H) = \frac{d \ln(|\Delta S_{max}|)}{d \ln(H)} \quad (7)$$

where ΔS_{max} is the maximum magnetic entropy change and n is an exponent related to magnetic order [37]. For a ferromagnet undergoing the second-order phase transition, n tends to 1 and is magnetic-field independent at temperatures $T \ll T_C$ but it tends to 2 at temperatures $T \gg T_C$ and reaches a minimum value equal to 2/3 at T_C [38]. However, the recent experiments exhibit deviation from $n = \frac{2}{3}$ in the soft magnetic amorphous alloys. Therefore, a new relationship between the exponent n at T_C and the critical exponents of second-order phase transition materials has been established as $n(T_C) = 1 + \frac{\beta - 1}{\beta + \gamma}$ [39]. Fig. 4(a) shows the temperatures dependence of n and a. It can be found that the value of n reaches 1.2 and exceeds 1.6 far below and above T_C, respectively, basically consistent with the universal law of n-change [40,41]. However, note that the value of $n = 0.879$ at T_C reveals an obvious deviation from $n = 0.67$ for mean-field model. In addition, by using $\beta = 0.4799$ and $\gamma = 1.374$ obtained from the previous discussion, the value of n is determined to be 0.719, which also shows a slight discrepancy. Therefore, this abnormal behavior and inconsistency imply that these discrepancies are related with the Dy-doping. In connection with the previous discussion, the Dy^{3+} ion causes two notable variations: one is a large MCE and the other is the critical exponents which does not conform to any theoretical models. In order to understand the basic reason for it, we need to inspect the Dy^{3+} ion how to play a role in the magnetic system. This issue can be analyzed from two aspects: (1) Considering the size mismatch among Dy^{3+}, La^{3+} and Sr^{2+}, it causes ionic disorder on A-site sublattice and indirectly influent and change MnO_6 octahedron structure on B-site sublattice. A-site cationic disorder due to the mismatch among Dy^{3+}, La^{3+} and Sr^{2+} can be depicted and quantified with the variance of A-cation radius distribution σ^2 ($\sigma^2 = \langle r_A^2 \rangle - \langle r_A \rangle^2$; $\langle r_A^2 \rangle = \Sigma x_i r_i^2$, $\langle r_A \rangle = \Sigma x_i r_i$, x_i is the fractional occupancy of A-site ions, r_i is the corresponding ionic radius) [42,43]. The value σ^2 of LDSMO is 41.86×10^{-4} Å^2, more than two times larger than 18.66×10^{-4} Å^2 for the pristine LSMO. The change of MnO_6 octahedron results in the variation of Mn–O–Mn bond angles and Mn–O bond lengths which are responsible for the systemical FM formation through the double exchange interaction on B-site sublattice. From the previous reports and the present results, one can find that the ionic doping suppresses the double exchange interaction and decreases the systemical ferromagnetism. (2) In the view of large magnetic moment of Dy^{3+} ion (10.6 μ_B), A-site magnetic moments also influent B-site FM interaction. Moreover, with the increase of A-site ionic disorder, the pristine long-range FM coupling can be further broken. As the material is in the circumstance of application or removal of external magnetic field, tremendous changes of FM ordering degree would take place on B-site sublattice. It leads to the presence of large magnetic entropy change and notable MCE. Since that the Dy-substitution causes crystal lattice effect and magnetic disordering, the systemical magnetic phase transition becomes more complex. Multiple factors will influence the magnetic phase transitional process. Therefore, the critical exponents obtained in LDSMO are impossible to be depicted with standard theoretical models and naturally dissatisfy the normal variation.

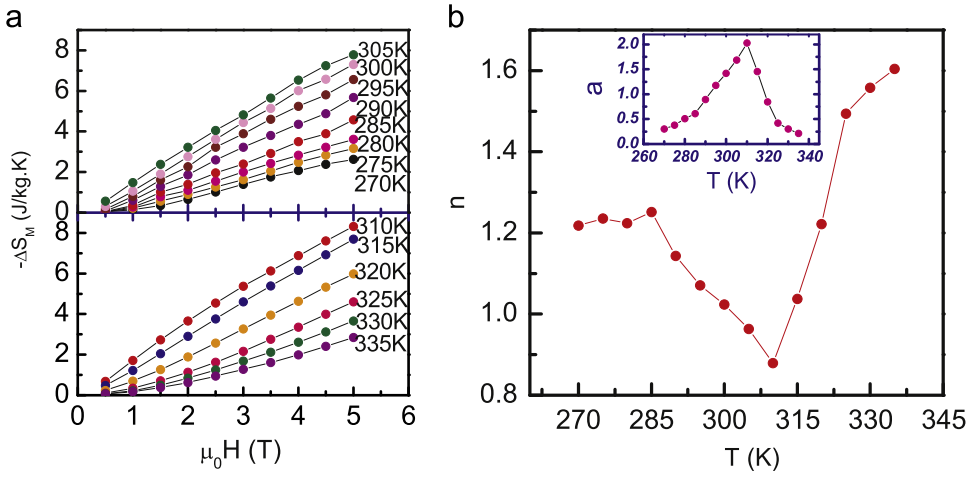

Fig. 4. (a) Magnetic field dependence of magnetic entropy change at different temperatures. (b) Temperature dependence of exponent x and inset shows the parameter a vs. temperatures.

4. Conclusion

In summary, we have studied in detail the magnetic and magnetocaloric effect for manganite LDSMO. A second-order transition from PM to FM phase has been observed. Large magnetic entropy change occurs at 307 K near room temperature. The values of magnetic entropy change and RCP are large enough for it to be applied in magnetic refrigeration. The critical exponents β, γ and δ are deduced by using the scaling law and Widom scaling relation and their reliability has been also confirmed with the scaling hypothesis. However, we found that these values of critical exponents did not belong to the common university classes. In connection with the crystal lattice effect due to Dy-substitution and large magnetic moment of Dy^{3+} ion, we think that the induced lattice disordering and magnetic disordering promote the formation of large MCE and exacerbate the complexity of a continuous PM–FM phase transition in the present material.

Acknowledgment

This work was supported by the National Nature Science Foundation of China (Grant nos. 11574322, 11204131, 11204270 and U1332140) and the Foundation for Users with Potential of Hefei Science Center (CAS) through Grant no. 2015HSC-UP001.

References

[1] K.A. Gschneidner Jr., V.K. Pecharsky, A.O. Tsokol, Recent developments in magnetocaloric materials, Rep. Prog. Phys. 68 (2005) 1479.
[2] N.A. de Oliveira, P.J. vonRanke, Theoretical aspects of the magnetocaloric effect, Phys. Rep. 489 (2010) 89.
[3] V. Franco, J.S. Blazquez, B. Ingale, A. Conde, The magnetocaloric effect and magnetic refrigeration near room temperature: materials and models, Annu. Rev. Mater. Res. 42 (2012) 305.
[4] V.K. Pecharsky, K.A. Gschneidner, Giant magnetocaloric effect in $Gd_5(Si_2Ge_2)$, Phys. Rev. Lett. 78 (1997) 4494.
[5] F.X. Hu, B.G. Shen, J.R. Sun, Z.H. Cheng, G.H. Rao, X.X. Zhang, Influence of negative lattice expansion and metamagnetic transition on magnetic entropy change in the compound $LaFe_{11.4}Si_{1.6}$, Appl. Phys. Lett. 78 (2001) 3675.
[6] K.A. Gschneidner Jr., V.K. Pecharsky, Magnetocaloric materials, Annu. Rev. Mater. Sci. 387 (2000) 30.
[7] Z.B. Guo, Y.W. Du, J.S. Zhu, H. Huang, W.P. Ding, D. Feng, Large magnetic entropy change in perovskite-type manganese oxides, Phys. Rev. Lett. 78 (1997) 1142.
[8] M.H. Phan, S.C. Yu, Review of the magnetocaloric effect in manganite materials, J. Magn. Magn. Mater. 308 (2007) 325.
[9] Manh-Huong Phan, Seong-Cho Yu, Nam Hwi Hur, Yoon-Hee Jeong, Large magnetocaloric effect in a $La_{0.7}Ca_{0.3}MnO_3$ single crystal, J. Appl. Phys. 96 (2004) 1154.
[10] R. Skini, A. Omri, M. Khlifi, E. Dhahri, E.K. Hlil, Large magnetocaloric effect in lanthanum-deficiency manganites $La_{0.8-x}Ca_{0.2}MnO_3$ ($0.00 \le x \le 0.20$) with a first-order magnetic phase transition, J. Magn. Magn. Mater. 364 (2015) 5.
[11] Kalipada Das, Tapas Paramanik, I. Das, Large magnetocaloric effect in $Ln_{0.5}Ca_{0.5}MnO_3$ (Ln=Gd, DY) compounds: consequence of magnetic precursor effect of rare earth ions, J. Magn. Magn. Mater. 374 (2015) 707.
[12] Renwen Li, Wei Tong, Li Pi, Yuheng Zhang, Coexistence of large magnetoresistance and magnetocaloric effect in monovalent doped manganite $La_{0.5}Ca_{0.4}Li_{0.1}MnO_3$, J. Magn. Magn. Mater. 355 (2014) 276.
[13] M. Wali, R. Skini, M. Khlifi, E. Dhahri, E.K. Hlil, A giant magnetocaloric effect with a tunable temperature transition close to room temperature in Na-deficient $La_{0.8}Na_{0.2-x}MnO_3$ manganites, Dalton Trans. 44 (2015) 12796.
[14] Jiyu Fan, Li Pi, Lei Zhang, Wei Tong, Langsheng Ling, Bo Hong, Yangguang Shi, Weichun Zhang, Di Lu, Yuheng Zhang, Magnetic and magnetocaloric properties of perovskite manganite $Pr_{0.55}Sr_{0.45}MnO_3$, Physica B 406 (2011) 2289.
[15] Jiyu Fan, Li Pi, Lei Zhang, Wei Tong, Langsheng Ling, Bo Hong, Yangguang Shi, Weichun Zhang, Di Lu, Yuheng Zhang, Investigation of critical behavior in $Pr_{0.55}Sr_{0.45}MnO_3$ by using the field dependence of magnetic entropy change, Appl. Phys. Lett. 98 (2011) 072508.
[16] A. Urushibara, Y. Moritomo, T. Arima, A. Asamitsu, G. Kido, Y. Tokura, Phys. Rev. B 51 (1995) 14103.
[17] J.B. Goodenough, Insulator-metal transition and giant magnetoresistance in $La_{1-x}Sr_xMnO3$, Phys. Rev. 100 (1955) 564.
[18] Y. Tokura, Y. Tomioka, Colossal magnetoresistive manganites, J. Magn. Magn. Mater. 200 (1999) 1.
[19] M.H. Phan, M.B. Morales, N.S. Bingham, H. Srikanth, Phase coexistence and magnetocaloric effect in $La_{5/8-y}Pr_yCa_{3/8}MnO_3$ ($y = 0.275$), Phys. Rev. B 81 (2010) 094413.
[20] J. Kubler, Theory of Itinerant Electron Magnetism, Clarendon Press, Oxford, 2000.
[21] M.E. Fisher, The theory of equilibrium critical phenomena, Rep. Prog. Phys. 30 (1967) 615.
[22] E.V. Sampathkumaran, I. Das, Magnetoresistance anomalies in the Gd-based alloys, Phys. Rev. B 51 (1995) 8631.
[23] R. Mallik, E.V. Sampathkumaran, Magnetic precursor effects in Gd based intermetallic compounds, Phys. Rev. B 58 (1998) 9178.
[24] E. Bruck, Developments in magnetocaloric refrigeration, J. Phys. D: Appl. Phys. 38 (2005) R381.
[25] V. Pecharsky, K. Gschneidner, Some common misconceptions concerning magnetic refrigerant materials, J. Appl. Phys. 90 (2001) 4614.
[26] V. Franco, A. Conde, Scaling laws for the magnetocaloric effect in second order phase transitions: from physics to applications for the characterization of materials, Int. J. Refrig. 33 (2010) 465.
[27] Lisha Xu, Jiyu Fan, Yan Zhu, Yangguang Shi, Lei Zhang, Pi Li, Yuheng Zhang, Daning Shi, Critical behavior and long-range ferromagnetic order in perovskite manganite $Nd_{0.55}Sr_{0.45}MnO_3$, Mater. Res. Bull. 73 (2016) 187.
[28] R. Mnassri, N. Chniba-Boudjada, A. Cheikhrouhou, 3D-Ising ferromagnetic characteristic and magnetocaloric study in $Pr_{0.4}Eu_{0.2}Sr_{0.4}MnO_3$ manganite, J. Alloys Compd. 640 (2015) 183.
[29] S.K. Banerjee, On a generalised approach to first and second order magnetic transitions, Phys. Lett. 12 (1964) 16.
[30] C.M. Bonilla, J. Herrero-Albillos, F. Bartolome, L.M. Garcia, M. Parra-Borderias, V. Franco, Universal behavior for magnetic entropy change in magnetocaloric materials: an analysis on the nature of phase transitions, Phys. Rev. B 81 (2010) 224424.
[31] V. Franco, J.S. Blazquez, A. Conde, Field dependence of the magnetocaloric effect in materials with a second order phase transition: a master curve for the magnetic entropy change, Appl. Phys. Lett. 89 (2006) 222512.
[32] H.E. Stanley, Introduction to Phase Transitions and Critical Phenomena, Oxford University Press, London, 1971.
[33] A. Arrott, Criterion for ferromagnetism from observations of magnetic isotherms, Phys. Rev. 108 (1957) 1394.
[34] B. Widom, Equation of state in the neighborhood of the critical point, J. Chem. Phys. 43 (1965) 3898.
[35] Jiyu Fan, Langsheng Ling, Bo Hong, Li Pi, Yuheng Zhang, Critical properties of the perovskite manganite $La_{0.1}Nd_{0.6}Sr_{0.3}MnO_3$, Phys. Rev. B 81 (2010) 144426.
[36] S.N. Kaul, Static critical phenomena in ferromagnets with quenched disorder, J. Magn. Magn. Mater. 53 (1985) 5.
[37] V. Franco, A. Conde, Scaling laws for the magnetocaloric effect in second order phase transitions: from physics to applications for the characterization of materials, Int. J. Refrig. 33 (2010) 465.
[38] H. Oesterreicher, F.T. Parker, Magnetic cooling near Curie temperatures above 300 K, J. Appl. Phys. 55 (1984) 4334.
[39] V. Franco, A. Conde, J.M. Romero-Enrique, J.S. Blazquez, A universal curve for the magnetocaloric effect: an analysis based on scaling relations, J. Phys.: Condens. Matter 20 (2008) 285207.
[40] R. Mnassi, N. Chniba-Boudjada, A. Cheikhrouhou, J. Alloys Compd. 640 (2015) 183.
[41] R. Caballero-Flores, N.S. Bingham, M.H. Phan, M.A. Torija, C. Leighton, V. Franco, A. Conde, T.L. Phan, S.C. Yu, H. Srikanth, Magnetocaloric effect and critical behavior in $Pr_{0.5}Sr_{0.5}MnO_3$: an analysis of the validity of the Maxwell relation and the nature of the phase transitions, J. Phys.: Condens. Matter 26 (2014) 286001.
[42] L.M. Rodriguez-Martinez, J.P. Attfield, Cation disorder and size effects in magnetoresistive manganese oxide perovskites, Phys. Rev. B 54 (1996) R15622.
[43] D. Louca, T. Egami, E.L. Brosha, H. Röder, A.R. Bishop, Local Jahn–Teller distortion in $La_{1-x}Sr_xMnO3$ observed by pulsed neutron diffraction, Phys. Rev. B 56 (1997) R8475.
[44] K. Huang, Statistical Mechanics, 2nd ed., Wiley, New York, 1987.
[45] A. Rostamnejadi, M. Venkatesan, P. Kameli, H. Salamati, J.M.D. Coey, Magnetocaloric effect in $La_{0.67}Sr_{0.33}MnO_3$ manganite above room temperature, J. Magn. Magn. Mater. 323 (2011) 2214.
[46] P. Lampen, N.S. Bingham, M.H. Phan, H. Kim, M. Osofsky, A. Pique, T.L. Phan, S.C. Yu, H. Srikanth, Impact of reduced dimensionality on the magnetic and magnetocaloric response of $La_{0.7}Ca_{0.3}MnO_3$, Appl. Phys. Lett. 102 (2013) 062414.
[47] D.T. Morelli, A.M. Mance, J.V. Mantese, A.L. Micheli, Magnetocaloric properties of doped lanthanum manganite films, J. Appl. Phys. 79 (1996) 373.
[48] M.H. Phan, S.C. Yu, N.H. Hur, Excellent magnetocaloric properties of $La_{0.7}Ca_{0.3-x}Sr_xMnO_3$ ($0.05 \le x \le 0.25$) single crystals, Appl. Phys. Lett. 86 (2005) 072504.
[49] M.H. Phan, H.X. Peng, S.C. Yu, Giant magnetoimpedance effect in ultrasoft FeAlSiBCuNb nanocomposites for sensor applications, J. Appl. Phys. 97 (2005) 10M306.